



Fatigue crack paths and properties in A356-T6 aluminum alloy microstructurally modified by friction stir processing under different conditions

A. Tajiri

*Murata Machinery, Ltd., Japan
akiko.tajiri@jbb.muratec.co.jp*

Y. Uematsu, T. Kakiuchi

*Gifu University, Japan
yuematsu@gifu-u.ac.jp*

Y. Suzuki

*Okuma Corp., Japan
mail@yahoo.com*

ABSTRACT. A356-T6 cast aluminum alloy is a light weight structural material, but fatigue crack initiates and propagates from a casting defect leading to final fracture. Thus it is important to eliminate casting defects. In this study, friction stir processing (FSP) was applied to A356-T6, in which rotating tool with probe and shoulder was plunged into the material and travels along the longitudinal direction to induce severe plastic deformation, resulting in the modification of microstructure. Two different processing conditions with low and high tool rotational speeds were tried and subsequently fully reversed fatigue tests were performed to investigate the effect of processing conditions on the crack initiation and propagation behavior. The fatigue strengths were successfully improved by both conditions due to the elimination of casting defects. But the lower tool rotational speed could further improve fatigue strength than the higher speed. EBSD analyses revealed that the higher tool rotational speed resulted in the severer texture having detrimental effects on fatigue crack initiation and propagation resistances.

KEYWORDS. Fatigue; Cast aluminium alloy; Friction stir processing; Texture.

INTRODUCTION

Al-Mg-Si cast aluminum (Al) alloy, A356-T6, is widely used for mechanical components due to its light weight and near-net-shape manufacturability. Some investigations on fatigue behavior of this alloy have revealed that fatigue crack generally initiated from casting defects [1-3]. It is well known that the crack initiation from defects shorten the fatigue life of component because fatigue crack initiation life becomes very short. Thus, removing casting defects is beneficial for improving fatigue life, but the elimination of defects by the innovation of casting technique is difficult.

Recently, friction stir processing (FSP) technique draws attention as a microstructural modification technique. In the FSP process, rotating tool with shoulder and probe is plunged into the material and travels leaving severely deformed area behind the tool. FSP was applied to cast Al and magnesium (Mg) alloys, and it has been reported that casting defects, such as porosities and large grains, are successfully removed [4-6]. Consequently, it has been revealed that fatigue strengths of cast Al or Mg alloys could be improved by the application of FSP [5, 7, 8].

It is well known that the fatigue properties are sensitive to the microstructures. It is believed that FSP would leave strong texture behind the tool, and the texture would be dependent on the FSP conditions. However, the effects of texture on fatigue properties, such as crack initiation and propagation resistances, are not clear. In this study, FSP was applied to A356-T6 under two different processing conditions, where the tool rotational speed was changed at the fixed tool traveling speed. Subsequently, fully reversed plane bending fatigue tests had been performed to investigate the effect of processing conditions on the crack initiation and growth behavior.

EXPERIMENTAL PROCEDURE

The material used is T6-treated A356 cast Al alloy. The chemical composition (wt. %) is as follows, Si: 6.66, Mg: 0.383, Fe: 0.153, Ni: 0.009, Cr: 0.002, Sn: 0.002, Al: balance. The microstructure of the as-received material is shown in Fig.1. Typical dendrite structures are seen. It should be noted that large casting defects are recognized in the microstructure as shown by the arrows in the figure. Specimen blanks with the thickness of 5 mm were cut from the ingots and subsequently friction stir processed (FSPed), from which plane bending fatigue specimens were machined. The FSP direction corresponds to the longitudinal direction of the specimen. To remove stress concentration sites, both the upper and lower surfaces were removed 0.3 and 0.7 mm in depth, respectively. Before fatigue test, the surface of the gauge section was mechanically polished using #2000 grade emery paper followed by buff-finishing.

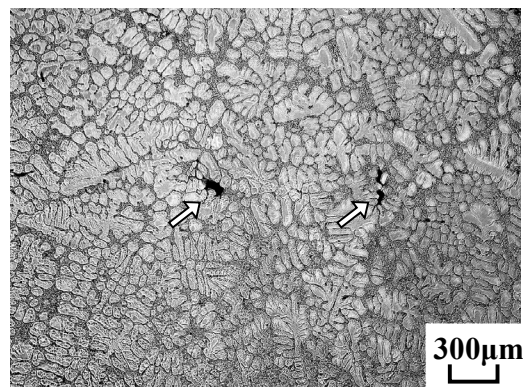


Figure 1: Microstructure of as-received material. Arrows indicate casting defects.

The FSP tool consists of concave shoulder with a diameter of 14 mm and M6-threaded probe with a length of 4.7 mm. The tool travelling speed was fixed at 150 mm/min. It is considered that the development of texture will be affected by the strain rate. Accordingly, the tool rotational speed was set to be 500 and 1000 rpm to investigate fatigue properties in the FSPed specimens fabricated under low and high strain rates. Hereafter, the specimens are designated as L (Low strain rate) and H (High strain rate) samples.

Fatigue tests had been conducted using resonance-type plane bending fatigue testing machine, SIMADZU TB-10, at a test frequency $f=33.3\text{Hz}$ and load ratio $R=-1$ (fully reversed bending). The hardness was measured by micro-Vickers hardness tester at a load of 2.49 N and dwell time of 30 s.

RESULTS

Microstructure

The cross section of FSP line in L and H specimens are revealed in Fig.2. Dendrite structures were broken-up by the stirring action during FSP in the stir zone (SZ), and porosities shown in Fig.1 were not recognized in the SZ. The so-called onion ring patterns are clearly seen in H specimen while they were partially formed in L specimen. It



should be noted that onion ring patterns are more strongly formed under high strain rate FSP condition (1000 rpm).

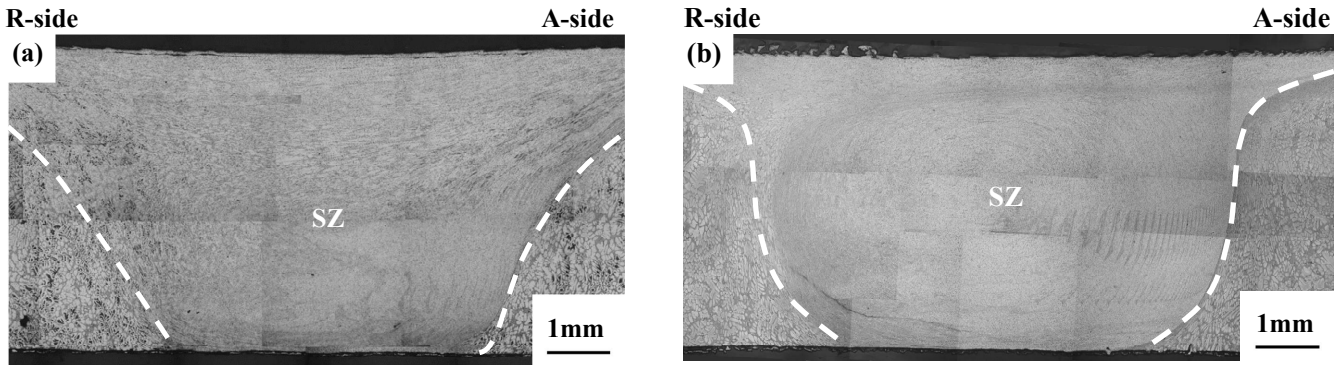


Figure 2: Macroscopic structure observed on the cross section of stir zone; (a) L specimen, (b) H specimen.

Fatigue properties

The tensile strengths of the as-received, L and H specimens are 218, 199 and 215 MPa, respectively. L specimen has slightly lower ultimate strength, but the tensile strength is insensitive to the tool rotational speed. The *S-N* diagram is shown in Fig. 3, in which high cycle fatigue strengths were highly improved by FSP compared with the as-received material. It should be noted that the FSP under lower rotational speed had resulted in the higher fatigue strength than that under higher speed. Fig. 4 reveals the fracture surface near crack initiation site in the as-received material. Large casting defect is recognized at the crack initiation site, indicating the typical fatigue crack initiation mechanism of A356 cast Al alloy. On the contrary, casting defects were not found in L and H specimens as indicated in Fig.5, showing fracture surfaces near crack initiation sites. It could be concluded that casting defects were successfully eliminated by both FSPs under low and high tool rotational speeds. Consequently, the increase of fatigue strengths in the FSPed specimens could be mainly attributed to the transition of crack initiation mechanism from defect-dominated to cyclic-slip-dominated crack initiation.

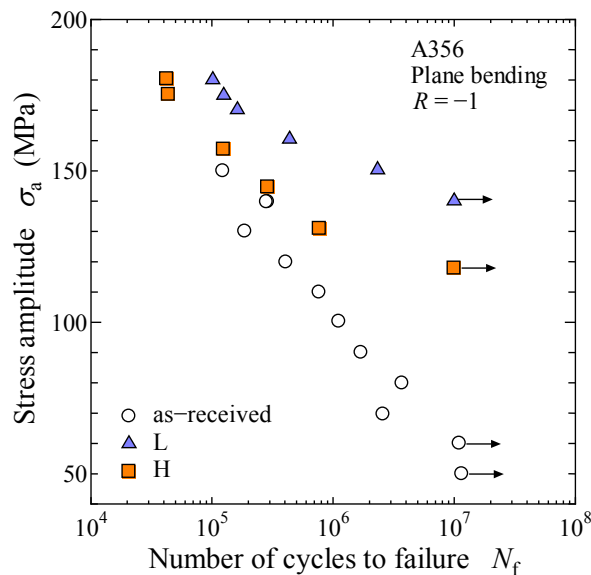


Figure 3: *S-N* diagram.

Small fatigue crack growth behavior was monitored by a plastic replication technique. A fatigue test was periodically terminated, and the shape of fatigue crack was copied to the plastic replica film. Consequently, fatigue crack growth rates, da/dN , was measured from the crack length as a function of number of cycles. Fig. 6 shows the relationship between da/dN and maximum stress intensity factor, K_{max} . In this case, K_{max} was calculated assuming the aspect ratio of surface

crack as 0.5 (semicircular crack), and using Newman-Raju equation [9]. It should be noted that crack growth rates become higher in the as-received, L and H specimens in the increasing order. Based on the $S-N$ diagram (Fig.3), it can be said that the crack initiation resistance of the as-received material was improved by FSP, while $da/dN-K_{max}$ relationship (Fig.6) reveals FSP has detrimental effects on the crack growth resistance.

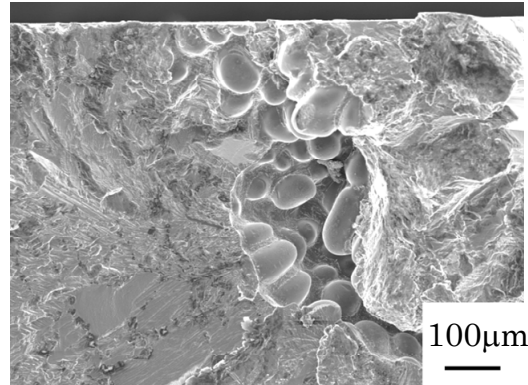


Figure 4: Fracture surfaces near crack initiation site in the as-received material ($\sigma_a=140\text{MPa}$, $N_f=2.81\times 10^5$).

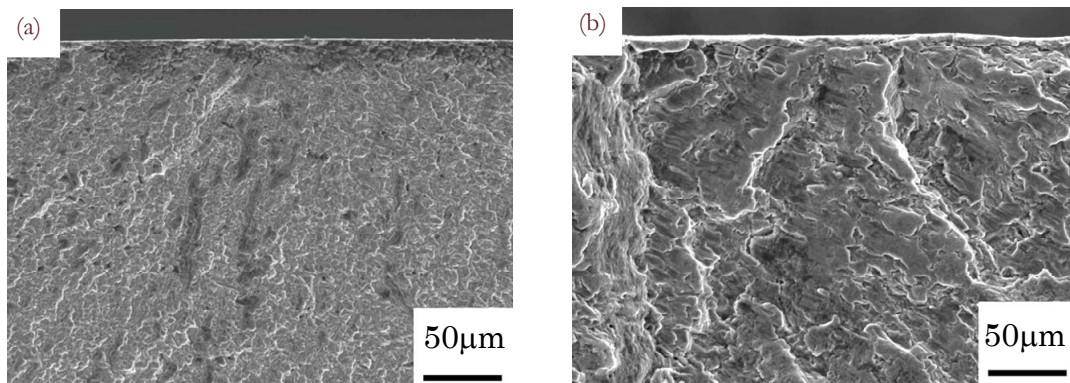


Figure 5: Fracture surfaces near crack initiation site in the FSPed materials; (a) L specimen ($\sigma_a=170\text{MPa}$, $N_f=1.62\times 10^5$), (b) H specimen ($\sigma_a=180\text{MPa}$, $N_f=4.23\times 10^4$).

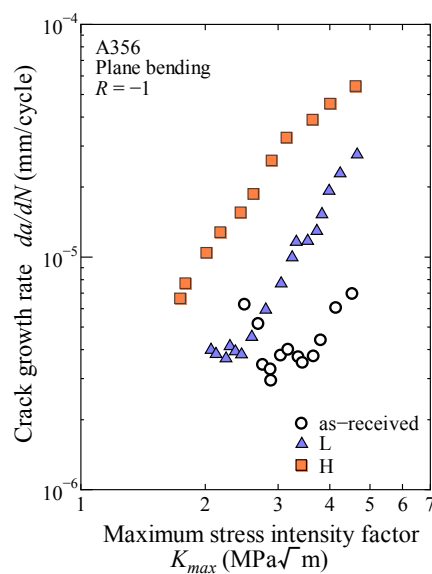


Figure 6: Relationship between crack growth rate, da/dN , and maximum stress intensity factor, K_{max} .

DISCUSSION

Higher crack initiation resistances of the FSPed specimens could be easily attributed to the elimination of casting defects as clearly revealed from the fractographic analyses near crack initiation sites (Fig.4 and 5). But the reason for the lower crack growth resistance of FSPed specimens is unclear. The macroscopic appearances of the crack paths in the as-received, L and H specimens are shown in Fig.7. Fatigue crack, initiated from casting defect, grew macroscopically perpendicular to the loading direction in the as-received specimen (Fig.7(a)). On the contrary, the crack paths are macroscopically curved in L and H specimens. Especially, in H specimen, the shape of fatigue crack path corresponds well with the onion ring patterns in Fig.2(b). It indicates that the fatigue crack growth path is affected by the microstructure, such as texture, induced by severe plastic deformation by FSP.

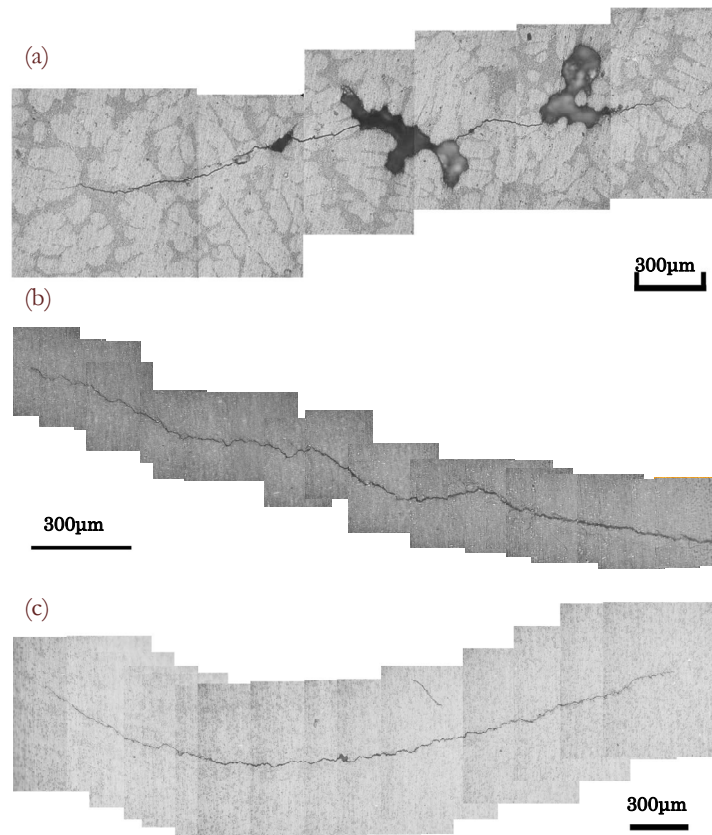


Figure 7: Crack growth paths just before final fracture: (a) as-received, $N=0.78N_f$, (b) L specimen, $N=0.98N_f$, (c) H specimen, $N=0.92N_f$. N_f is number of cycles to failure.

To investigate the effect of texture induced by FSP on the fatigue properties, EBSD analyses were performed along the fatigue crack path. Fig. 8(a) indicates the macroscopic fatigue crack path of L specimen. EBSD analyses were conducted in the areas (A) ~ (F) in Fig.8(a), and corresponding pole figures are shown in Fig.8(b). FCC unit cells in accordance with pole figures are also indicated in Fig.8(b). The macroscopic fatigue crack path of H specimen, pole figures and FCC unit cells are shown in Fig.9. Texture evolution is clear along the crack path in H specimen (Fig.9(b)). Morita et al. investigated texture evolution in wrought Al-Mg-Si alloy FSW joint, and proposed the rotation of unit cells around the probe as shown in Fig.10 [10]. Fig. 11 indicates the schematic illustration of the rotation of unit cells around the probe, resulting in the texture evolution in A356. The unit cell rotation in A356 is slightly different from that in wrought Al-Mg-Si alloy (Fig.10), due to the different processing conditions and chemical composition. It is clear that the fatigue crack path is dependent on the orientations of unit cells. In L specimen, however, unit cell rotations are less clearer as shown in Fig.8(b) than in H

specimen, indicating that the texture evolution is weaker under lower strain rate. Consequently, it could be concluded that H specimen has stronger texture. As shown in Fig.3, H specimen exhibited lower fatigue strengths than L specimen due to lower crack growth resistance (Fig.6). The lower resistance could be attributed to the stronger texture induced by FSP under higher strain rate. It is concluded that the elimination of casting defects is mandatory to improve fatigue strength of the as-received cast Al alloy, and in addition, FSP condition with weaker texture could give further increase of fatigue strength.

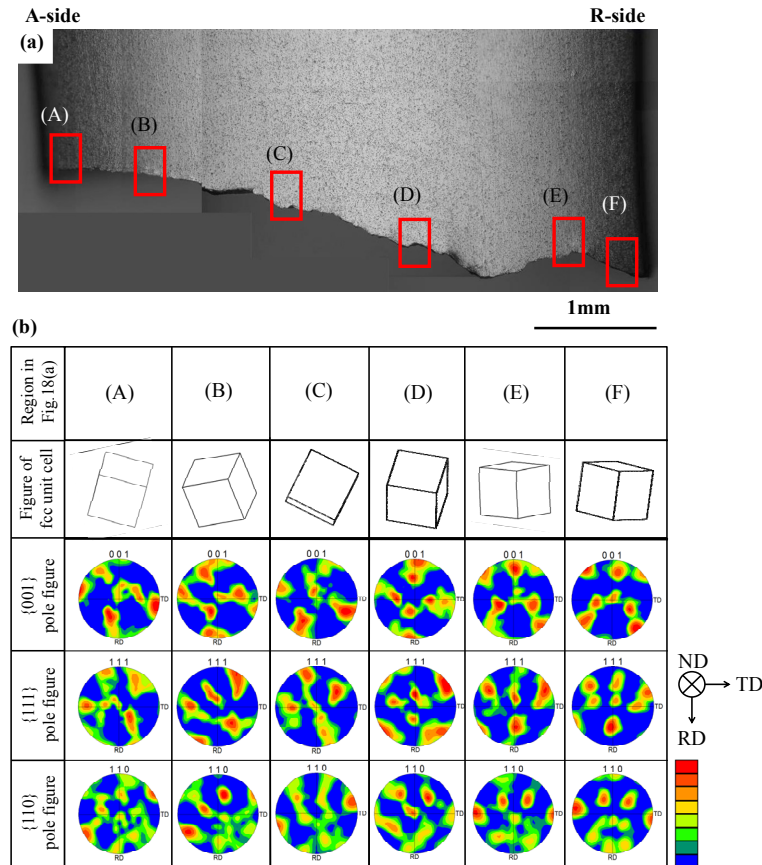


Figure 8: EBSD analysis results along crack path in L specimen: (a) Fatigue crack growth path, (b) Pole figures at the rectangular regions in (a).

CONCLUSION

FSP was applied to T6-treated A356 Al alloy under two different FSP conditions with low and high tool rotational speeds. The plane bending fatigue tests were conducted to investigate the effect of FSP conditions on fatigue properties. EBSD analyses were performed to figure out the texture evolution. The conclusions are as follows.

- (1) Casting defects were successfully removed by both FSP conditions. Clear onion ring patterns were fully developed under high tool rotational speed, while onion rings were partially formed near the top of the probe under low speed.
- (2) The fatigue strengths of FSP specimens were improved compared to the as-cast specimen, due to the elimination of casting defects. FSP under lower tool rotational speed could further improve fatigue strength than the higher speed.
- (3) L specimens exhibited higher crack initiation and growth resistances than H specimen. The higher resistances could be attributed to the weaker texture evolution under lower strain rate.

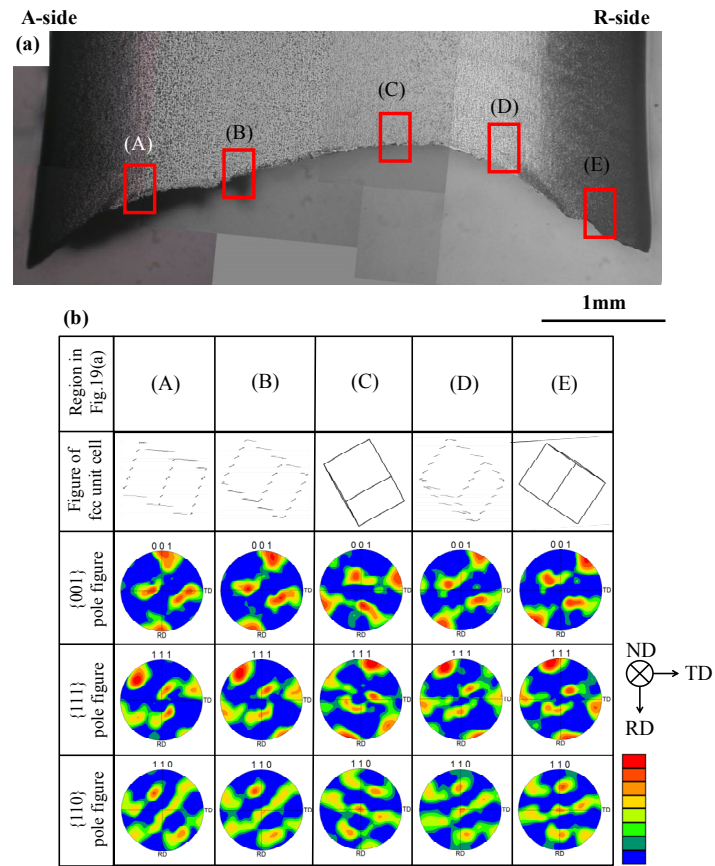


Figure 9: EBSD analysis results along crack path in H specimen: (a) Fatigue crack growth path, (b) Pole figures at the rectangular regions in Fig.(a).

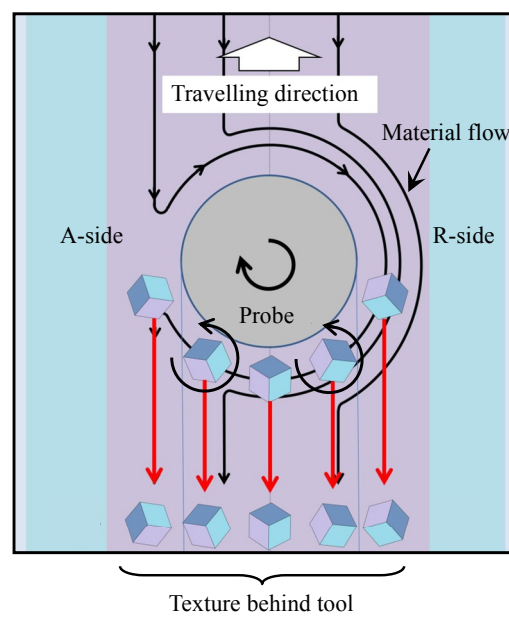


Figure 10: Schematic illustration of material flow around the tool and texture behind tool in Al-Mg-Si FSW joint [10].

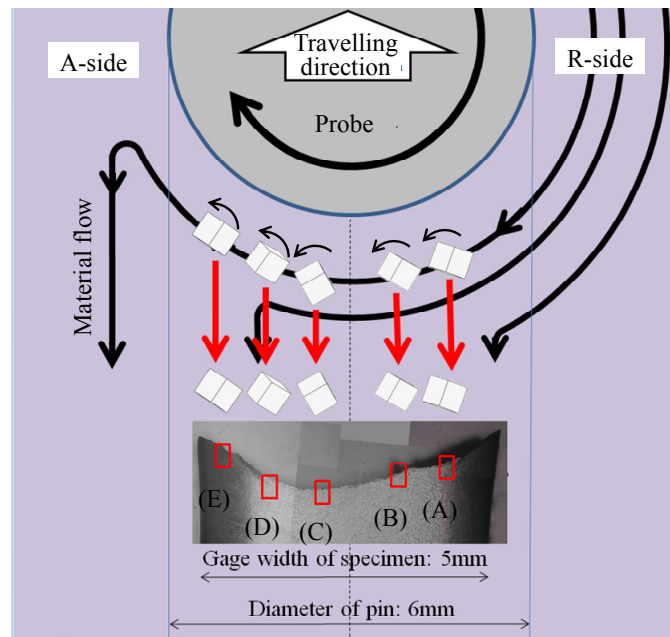


Figure 11: Schematic illustration of texture behind tool in A356 and fatigue crack path.

REFERENCES

- [1] Wang, Q.G., Apelian, D., Lados, D.A., Fatigue behavior of A356-T6 aluminum cast alloys, Part I. Effect of casting defects, *J. Light Metals*, 1 (2001) 73-84.
- [2] Tokaji, K., Notch fatigue behaviour in a Sb-modified permanent-mold cast A356-T6 aluminium alloy, *Mater. Sci. Eng.*, A396 (2005) 333-340.
- [3] Tajiri, A., Nozaki, T., Uematsu, Y., Kakiuchi, T., Nakajima, M., Nakamura, Y., Tanaka, H., Fatigue limit prediction of large scale cast aluminum alloy A356, *Procedia Mater. Sci.*, 3 (2014) 924-929.
- [4] Santella, M.L., Engstrom, T., Storjohann, D., Pan, T.Y., Effects of friction stir processing on mechanical properties of the cast aluminum alloys A319 and A356, *Scripta Materialia*, 53 (2005) 201-206.
- [5] Uematsu, Y., Tokaji, K., Fatigue behaviour of friction stir processed cast aluminium and magnesium alloys, *Mater. Sci. Forum*, 638-642 (2010) 3727-3730.
- [6] Cui, G.R., Ni, D.R., Ma, Z.Y., Li, S.X., Effects of friction stir processing parameters and in situ passes on microstructure and tensile properties of Al-Si-Mg Casting, *Metall. Mater. Trans.*, A45 (2014) 5318-5331.
- [7] Sharma, S.R., Ma, Z.Y., Mishra, R.S., Effect of friction stir processing on fatigue behavior of A356 alloy, *Scripta Materialia*, 51 (2004) 237-241.
- [8] Kapoor, R., Kandasamy, K., Mishra, R.S., Baumann, J.A., Grant G. Effect of friction stir processing on the tensile and fatigue behavior of a cast A206 alloy, *Mater. Sci. Eng.*, A561 (2013) 159-166.
- [9] Newman, J.C., Raju, I.S., Stress-intensity factor equations for cracks in three-dimensional finite bodies subjected to tension and bending loads, *NASA Technical Memorandum*, 83200 (1981) PR1-49.
- [10] Morita, T., Yamanaka, M., Microstructural evolution and mechanical properties of friction-stir-welded Al-Mg-Si joint, *Mater. Sci. Eng.*, A595 (2014) 196-204.